Biomedicine & Pharmacotherapy 156 (2022) 113882

Contents lists available at ScienceDirect

Biomedicine & Pharmacotherapy

journal homepage: www.elsevier.com/locate/biopha

Distinctive effects of SGLT2 inhibitors on angiogenesis in zebrafish embryos

Roope Huttunen [a], Annele Sainio [a], Anja Hjelt [a], Anna-Mari Haapanen-Saaristo [b], Jorma Määttä [a], Petri Rummukainen [a], Ilkka Paatero [b], Hannu Järveläinen [a,c,*]

[a] Institute of Biomedicine, University of Turku, Kiinamyllynkatu 10, 20520 Turku, Finland
[b] Turku Bioscience Centre, University of Turku and Åbo Akademi University, Tykistökatu 6, 20520 Turku, Finland
[c] Department of Internal Medicine, Satasairaala Central Hospital, Satakunta Hospital District, Sairaalantie 3, 28500 Pori, Finland

ARTICLE INFO

Keywords:
SGLT2 inhibitors
Diabetes
Angiogenesis
Zebrafish
Transcriptome
Amputation risk

ABSTRACT

Sodium glucose cotransporter 2 (SGLT2) inhibitor canagliflozin has been found to increase the risk for lower-limb amputations in type 2 diabetics about two-fold. Conversely, empagliflozin and dapagliflozin do not display a similar effect. A question arises whether the increased risk for minor amputations is associated only with canagliflozin or whether it is a class effect of SGLT2 inhibitors. Defective angiogenesis has a role in amputations. We compared the effects of empagliflozin, dapagliflozin and canagliflozin on angiogenesis *in vivo* using zebrafish model, and *in vitro* using human umbilical vein endothelial cells (HUVECs). The effects of SGLT2 inhibitors on the formation of intersegmental blood vessels (ISVs) of the zebrafish embryos were clarified. Additionally, transcriptome analysis was performed to explore whether putative angiogenesis-associated genes are differentially regulated by SGLT2 inhibitors. The effects of SGLT2 inhibitors on the viability of HUVECs were examined. We noticed that especially empagliflozin and also dapagliflozin significantly accelerated the formation of ISVs of zebrafish embryos. In contrast, canagliflozin was not able to stimulate ISV formation, and at high concentration, it was lethal to the embryos. Transcriptome analysis demonstrated that in empagliflozin-treated embryos compared to canagliflozin-treated embryos seven genes previously shown to contribute to angiogenesis were upregulated, and four downregulated. Canagliflozin at high concentrations, but not empagliflozin or dapagliflozin, decreased the viability of HUVECs and disrupted their capability to sprout. SGLT2 inhibitors differed in their effects on angiogenic processes in zebrafish embryos and on the viability of HUVECs suggesting that the risk of SGLT2 inhibitors for peripheral amputations likely differs.

1. Introduction

Long-term randomized controlled trials (RCTs) demonstrate that sodium glucose cotransporter 2 (SGLT2) inhibitors reduce the risk for cardiovascular and renal outcomes and all-cause mortality of type 2 diabetes patients [1–3]. SGLT2 inhibitors show cardiorenal benefits also in non-diabetic patients [4,5]. However, there is some heterogeneity between individual SGLT2 inhibitors in their effects on cardiovascular events [1, 6–9]. The mechanisms whereby SGLT2 inhibitors reduce the risk for cardiovascular and renal outcomes are currently not definitively known, but mechanisms beyond their effect on glycemic control are likely to play a major role [4,5,10]. The CANagliflozin cardioVascular Assessment Study (CANVAS) program demonstrated that the use of canagliflozin increases the risk for lower-limb amputation [8]. As such, both Food and Drug Administration (FDA) and European Medicines Agency (EMA) have warned about this rare but serious side effect and the possibility that this effect may be associated with all SGLT2 inhibitors, even if the association has not been observed in the large RCTs with empagliflozin and dapagliflozin [7, 11–13]. However, it has been discussed whether the increased risk for lower-limb amputation is a class effect produced by all SGLT2 inhibitors [14]. Interestingly, there are individual studies collectively suggesting that SGLT2 inhibitors differ in their effects on angiogenesis [15–17], and thereby their risk for amputations also likely differs. In this study, we compared the effects of empagliflozin, dapagliflozin and canagliflozin on angiogenesis *in vivo* using transgenic *kdrl:EGFP* zebrafish line [18] and *in vitro* using human umbilical vein endothelial cells (HUVECs).

* Corresponding author at: Institute of Biomedicine, University of Turku, Kiinamyllynkatu 10, 20520 Turku, Finland.
E-mail address: hanjar@utu.fi (H. Järveläinen).

https://doi.org/10.1016/j.biopha.2022.113882
Received 8 July 2022; Received in revised form 11 October 2022; Accepted 13 October 2022
Available online 18 October 2022

2. Material and methods

2.1. Zebrafish care and breeding

Adult *kdrl:EGFP* zebrafish [18] and fli1a:EGFP [32] were placed into mating tanks and after natural spawning, the fertilized eggs were collected and cultured in E3-medium (5 mM NaCl, 0.17 mM KCl, 0.33 mM CaCl2, 0.33 mM MgSO4) supplemented with 0.2 mM phenylthiourea (Sigma-Aldrich) at 28.5 °C. Thereafter, healthy green fluorescent protein (GFP) positive, 23 h post-fertilization (hpf) embryos were dechorionated and selected for the experiments. We performed the experiments under the license of MMM/465/712–93 issued by the Finnish Ministry of Agriculture and Forestry and carried out in the Zebrafish core facilities, Turku Bioscience. The zebrafish were a kind gift from Dr. Markus Affolter and Dr. Heinz-Georg Belting (University of Basel, Basel, Switzerland).

2.2. Angiogenesis quantification in vivo

The experiment overview is presented in Fig. 1a. Selected 23 hpf embryos were treated with the SGLT2 inhibitors empagliflozin, dapagliflozin and canagliflozin (Selleckchem, Houston TX, USA using drug concentrations of 1 μM, 10 μM, 50 μM, 100 μM, and 200 μM. The DMSO concentration was adjusted to 1 % in all treatments and concentrations. We maintained the embryos in an incubator at 28.5 C. At 27 hpf, the embryos were anesthetized with Tricaine (ethyl 3-aminobenzoate methane sulfonate salt, 200 mg/l) (Sigma-Aldrich, Saint Louis, Missouri, USA) and photographed with a stereomicroscope (Zeiss AxioZOOM.V16). We quantified the lengths of the last nine intersegmental blood vessels (ISVs) using ImageJ [19].

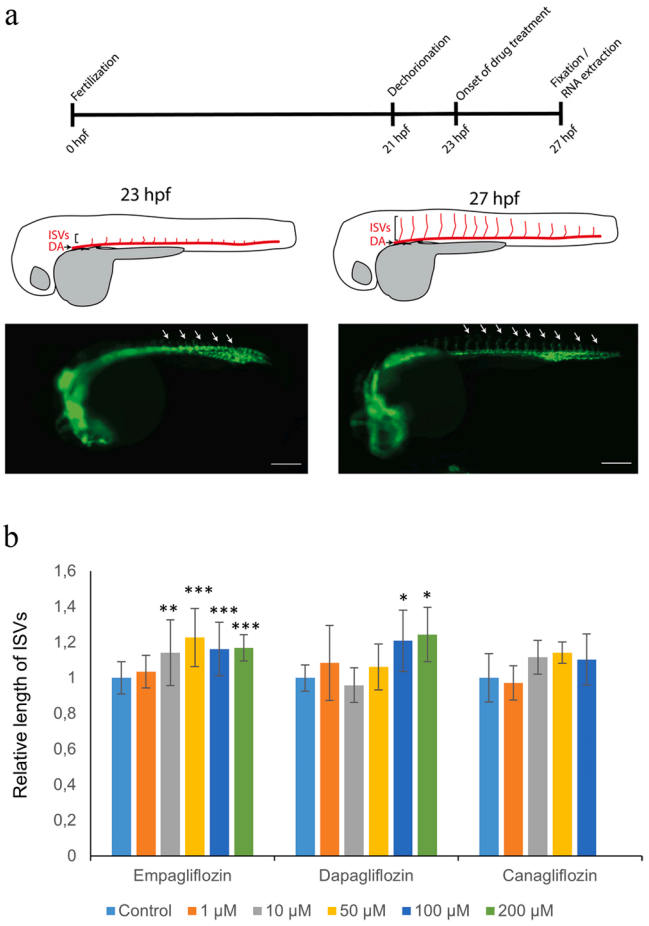

Fig. 1. a Overview on the zebrafish experiments with a diagram of the forming intersegmental blood vessels (ISVs) at two time points (23 hpf and 27 hpf), and microscope images of live embryos. The quantified ISVs are marked with white arrows. DA stands for dorsal aorta, hpf for hours post fertilization. Scale bar 200 μm (1b) Quantification of SGLT2 inhibitor-regulated ISV growth. The length of the vessels is given as relative lengths to control embryos. The number of embryos analyzed in 0, 1, 10, 50, 100, and 200 μM of SGLT2 inhibitors: empagliflozin n = 18, n = 18, n = 15, n = 12, n = 16, n = 14, respectively; dapagliflozin n = 7, n = 4, n = 8, n = 8, n = 9, and n = 6, respectively; canagliflozin n = 6, n = 4, n = 9, n = 8, n = 5, and n = 0, respectively. Data were analyzed with Dunnetts test and shown as mean +SD. ***P < 0.001, **P < 0.01, *P < 0.05.

Furthermore, time-lapse imaging of ISV formation in response to empagliflozin, dapagliflozin and canagliflozin was performed. First, the 22 hpf *roy, mitfa, fli1a:EGFP*^{y1} embryos were dechorionized and subsequently anaesthesized with Tricaine as above. Anesthesized embryos were mounted in optical 6-well plates on lateral orientation and in 0.7 % low-melting point agarose supplemented with test compounds and Tricaine (200 mg/l). After agarose had solidified, it was overlayed with 2 ml of E3-medium supplemented with test compounds and Tricaine. Samples were imaged at 28.5 ℃ using Nikon Eclipse Ti2 wide-field fluorescence microscope using 20× LD NA 0.45 objective, 475/28 nm LED illumination and GFP sPx 515/30 nm emission filter. Z-stack from each sample was taken with 10 min 15 s intervals and imaging was carried out for total of 26 cycles from ~23 hpf to ~27 hpf. After imaging, the images were processed using ImageJ [19] by background subtraction (rolling ball radius 25) and maximum projection along Z-axis. The length of ISVs in different time points were measured manually using ImageJ and segmented line tool, and elongation speed was calculated for each ISV.

To examine the effects of empagliflozin, dapagliflozin and canagliflozin on angiogenesis beyond 27 hpf, we analyzed ISV hypersprouting and quantified endothelial nuclei of 54 hpf *kdrl:EGFP* embryos as follows. Fixed 54 hpf *kdrl:EGFP* embryos were stained with 4 μg/ml of methyl green for 3 h in PBS + 0.2 % Tween-20 (PBSTw) at room temperature. After several washes with PBSTw, the embryos were mounted with low-melting point agarose in samples holder. Endothelial cell nuclei were identified through image processing of 3D datasets of vascular EGFP channel and general nuclear methyl green (MG) staining channel in ImageJ. In short, the background was removed (rolling ball radius 50) and EGFP and MG channels were multiplied with each other to highlight endothelial nuclei in a 32-bit floating image. The colocalization channel was subjected to background subtraction and pixel intensities converted back to 16-bit format and merge with EGFP and MG channels into a multi-channel 3D image stack. Finally, the number of endothelial nuclei in ISVs were counted manually and maximum Z-projections generated for presentation.

2.3. Image processing software

Images were processed using ImageJ [19], Arivis Vision 4D 3.5 (Arivis AG, Rostock, Germany) and Omero with Omero.figure (https://www.openmicroscopy.org/).

2.4. Transcriptome analysis and RNA-sequencing

The 27 hpf embryos (n = 5 per sample) were lysed and their total RNA was extracted with RNAeasy Mini Kit (QIAGEN, Hilden Germany) according to the manufacturer's instructions. The stranded mRNA sequencing analysis for control (DMSO), empagliflozin (50 μM), and canagliflozin (50 μM) (4 samples in each group) and the subsequent transcriptome analysis were performed at the Finnish Functional Genomics Center, Turku Bioscience (https://bioscience.fi/services/functional-genomics/services/). The data analysis was performed at the Medical Bioinformatics Center, Turku Bioscience (https://bioscience.fi/services/bioinformatics/).

2.5. Quantitative PCR

The angiogenesis-associated genes were validated using reverse transcriptase-quantitative polymerase chain reaction (RT-qPCR). Gene-specific primers for zebrafish (Table S1) were designed using NBCI Primer BLAST. RT-qPCR was performed using Sensifast™ cDNA Synthesis Kit (Meridian Bioscience, Cincinnati, Ohio, USA) and DyNAmo Flash SYBR Green qPCR Kit (Thermo Fisher Scientific) as triplicate reactions in CFX96 Touch Real-Time PCR Detection System (BioRad, Hercules, California, USA). Gene expression was normalized to ribosomal protein L13a (rpl13a) mRNA expression and quantified as relative to control using the relative ΔΔCq method [20].

2.6. Bioinformatic analysis of proteins encoded by the differentially regulated genes

We conducted a gene enrichment analysis with Panther (Protein ANalysis THrough Evolutionary Relationships) v14.0 Over-representation Test (http://geneontology.org/) [21] for the differentially regulated genes (Figure S1 A). The statistical testing of the significance of enrichment with Fisher's Exact Test was conducted with a false discovery rate (FDR) < 0.05. Thereafter, we performed the ontology analysis of the SGLT2 inhibitor regulated genes (Figure S1 B) using String database v11.0 (https://string-db.org/) with default settings [22].

2.7. Cell culture

The HUVECs were purchased from Lonza (cat no. C2519A, Basel, Switzerland) and cultured according to the manufacturer's instructions. The cells were tested negative for mycoplasma using MycoAlert™ Mycoplasma Detection Kit (Lonza) before the experiments.

2.8. Cell viability testing and imaging of tube-formation in vitro

The 3-(4,5-dimethylthiazol-2-yl)− 2,5-diphenyltetrazolium bromide (MTT) assay for HUVECs was performed according to the manufacturer's (Promega, Madison, WI, USA) protocol using 1, 10, and 50 μM of each SGLT2 inhibitor.

Also, the imaging of tubule sprouting was carried out using the same SGLT2 inhibitor concentrations as in the MTT assays. The formation of tube-like structures in HUVECs grown on Matrigel-coated 6-well dishes was photographed at 16 h with microscope using 4× objective (Olympus Leica, Tokyo, Japan).

2.9. Data analyses

The statistical significance between the different SGLT2 inhibitors on ISV formation was analyzed with Dunnett's multiple comparison test. The differential effect of SGLT2 inhibitors on ISV hypersprouting (yes/no scale) and the number of endothelial cell nuclei in the sprouts were analyzed using Fisher's exact test. The 90 % confidence interval for fraction of embryos displaying hypersprouting phenotype was generated using Wilson/Brown algorithm in GraphPad Prism 9. The RT-qPCR results were analyzed using multiple Student's t-test adjusting false discovery rate (Q) to 5 % using GraphPad Prism 6.05 software (GraphPad Software, La Jolla, California, USA). The significance of differences between the SGLT2 inhibitor treated HUVECs in the MTT assay *in vitro* was performed with one-tailed Student's t-test.

3. Results

3.1. Empagliflozin, dapagliflozin and canagliflozin differ in their effects on ISV formation in zebrafish

The SGLT2 inhibitors differed in their effects on stimulating the growth of ISVs in zebrafish embryos, *i.e.* angiogenesis (Fig. 1b). Empagliflozin treatment showed the greatest potency in stimulating ISV growth of zebrafish embryos' trunk. It increased the length of the ISVs statistically significantly already at the concentration of 10 μM. Dapagliflozin also increased the speed of sprouting of the ISVs of zebrafish embryos' trunk, although at higher concentrations (100 and 200 μM). In contrast, canagliflozin failed to stimulate the formation of ISVs, and at the concentration of 200 μM, it was lethal to the embryos.

Time-lapse analysis to examine the speed of ISV growth during 23–27 hpf further confirmed the finding above. Consistently with single time point analyses (Fig. 1b), the growth speed of ISVs was significantly faster upon treatment with empagliflozin and dapagliflozin than with DMSO control (Fig. 2). Canagliflozin failed this effect (Fig. 2). Interestingly, with empagliflozin the stimulation of angiogenesis as estimated with sprouting phenomenon was still evident beyond 27 hpf. As shown in Fig. 3, empagliflozin treated embryos displayed increased sprouting and formation of ectopic vascular branches at the time point 54 hpf. The same effect was not observed with dapagliflozin or canagliflozin (Fig. 3). To further examine the effect of empagliflozin, dapagliflozin and canagliflozin on angiogenesis beyond 27 hpf, we stained *kdrl:EGFP* transgenic embryos with nuclear dye and created a vascular specific nuclear signal channel by using co-localization analysis. The results showed that the cell number in ISVs was significantly increased in response to empagliflozin, but not with dapagliflozin or canagliflozin (Fig. 4). This implies that empagliflozin increased cell divisions of endothelial cells.

3.2. Early developmental processes in vivo are affected by SGLT2 inhibitors

To analyze potential differences in transcriptomic response induced by SGLT2 inhibitors, a comparison (FC > 2 and FDR < 0.05) in the gene expression profile between empagliflozin- and canagliflozin-treated embryos was conducted. The results showed that empagliflozin and canagliflozin differentially regulate the expression of 45 genes. Of these 45 genes, 33 were upregulated and 12 downregulated in response to empagliflozin compared to canagliflozin (Table 1).

We also performed gene enrichment analysis using Panther (Figure S 1A). The gene ontology molecular annotations detected various developmental steps including eye development and visual perception. Gene ontology analysis using String showed one known interaction from curated databases, namely interaction between fibronectin 1b (Fn1b) and matrilin 3a (Matn3a), and a few interactions based on, *e.g.* text mining (Figure S1 B). Similar to Panther, the results from String showed no direct indication in the regulation of angiogenesis.

3.3. Several angiogenesis-associated genes exhibit differential expression in response to empagliflozin and canagliflozin

As the bioinformatics pathway and the interaction analyses failed to provide clear answers, we carried out a detailed literature search on significantly altered genes. Of the upregulated genes, we found seven genes (Table 2A) that have earlier been shown to contribute to angiogenesis regulation, namely *ankyrin repeat domain 1b* (*ankrd1b*), *annexin A3a* (*anxa3a*), *atonal bHLH transcription factor 7* (*atoh*), *ceruloplasmin* (*cp*), *early growth response 1* (*egr1*), *fibronectin 1b* (*fn1b*), and *ferritin, heavy polypeptide-like 30* (*Zgc:173593*). Likewise, of the downregulated genes (Table2 B), four genes have previously been demonstrated to be involved in angiogenesis. These are *ankyrin repeat domain 37* (*ankrd37*), *cd36, cathepsin S* (*ctssb.1*), and *matrix metallopeptidase 13a* (*mmp13a*).

Of the seven significantly upregulated genes four genes could be validated by RT-qPCR, namely *ankrd1b*, *atoh7*, *cp*, and *zgc:173593* (Fig. 5). Regarding the four downregulated genes, three of them, *aknrd37, cd36*, and *ctssb1* had validated downregulation (Fig. 6).

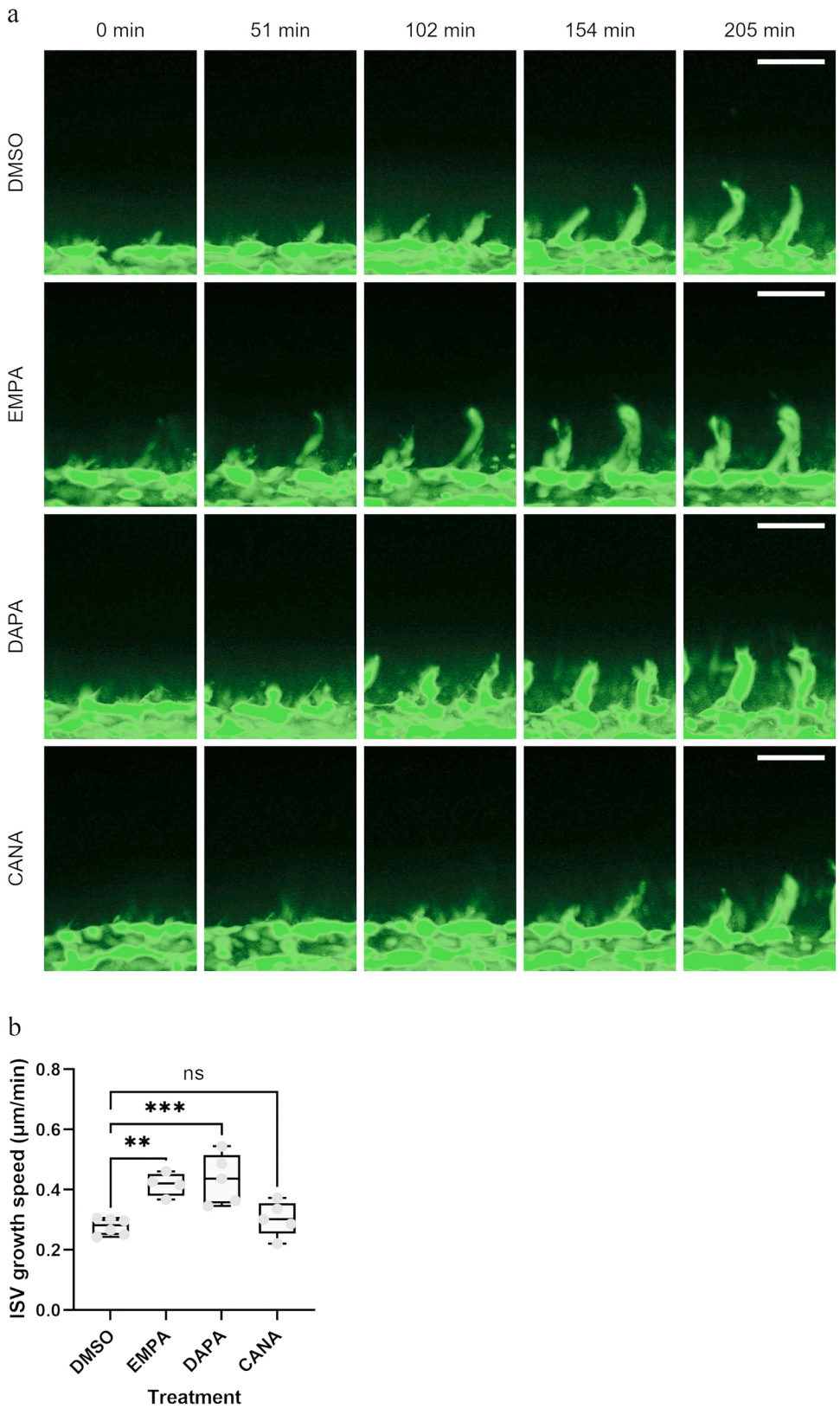

Fig. 2. a Transgenic *fli1a:EGFP, roy, mitfa* fish were anesthesized, immobilized in agarose and imaged from 23 hpf to 27 hpf. Maximum projections of the representative images from 0 to 205 min are shown. Scale bar 50 µm (2b) The elongation speed of ISVs was quantified and analyzed using one-way ANOVA and Dunnett's *post hoc* test. Average speed per embryo was used and are presented in the graph. DMSO [solvent control, n = 6 embryos (23 ISVs), EMPA (50 µM empagliflozin, n = 4 embryos (13 ISVs), DAPA (50 µM dapagliflozin, n = 5 embryos (18 ISVs), CANA (50 µM canagliflozin, n = 5 embryos (14 ISVs)]. ***P < 0.001, **P < 0.01, ns=non-significant.

3.4. Empagliflozin and canagliflozin differentially influence the viability and angiogenesis behavior of HUVECs in vitro

We treated HUVECs with SGLT2 inhibitors using concentrations of 1, 10, and 50 µM and assessed their viability with MTT assay (Fig. 7). In MTT assay, canagliflozin at concentrations of 10 and 50 µM significantly decreased the viability of HUVECs. We also examined the tube-forming capability of HUVECs *in vitro*. Here, treatment of HUVECs with 50 µM of canagliflozin completely disrupted their capability to form tube-like structures (Fig. 8).

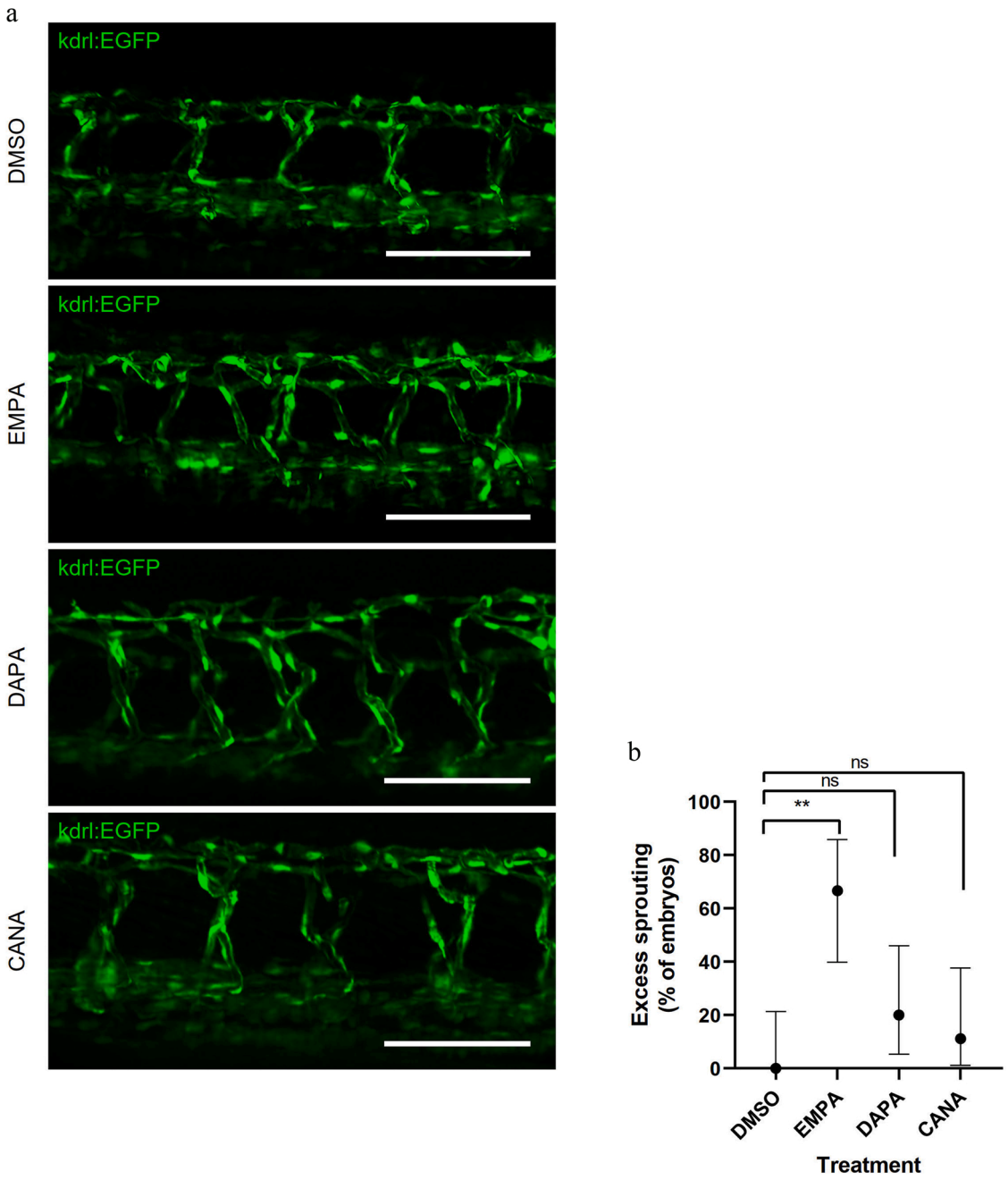

Fig. 3. a Transgenic *kdrl:EGFP* zebrafish embryos were treated with inhibitors from 23 hpf to 54 hpf and fixed. The samples were imaged with light-sheet fluorescence microscope. Representative images of the sprouting are shown. Scale bar 100 μm.(3b) Quantification of excess sprouting in the embryos. Statistical analysis using Fisher's exact test, error bars produced with Wilson/Brown algorithm. DMSO, n = 10 embryos; EMPA (50 μM empagliflozin), n = 9 embryos; DAPA (50 μM dapagliflozin), n = 10 embryos; CANA (50 μM canagliflozin), n = 9 embryos. **P < 0.01, ns=non-significant.

4. Discussion

Using a transgenic *kdrl:EGFP* zebrafish line, we show here that individual SGLT2 inhibitors have distinctive effects on angiogenesis *in vivo*. Specifically, we show here that especially empagliflozin and also dapagliflozin significantly accelerate the formation of ISVs of zebrafish embryos, while canagliflozin is not able to do the same, and at high concentration it is lethal to the embryos. Our results are in agreement with previous studies demonstrating that empagliflozin effectively enhances angiogenesis in the heart of diabetic mice [17] whereas canagliflozin decreases the ischemic hind-limb microvessel density in these animals [16]. Furthermore, various cardiovascular effects of SGLT2 inhibitors have been reviewed [23] and notably, canagliflozin often has different effects compared with others. Our results with HUVECs *in vitro* further show that canagliflozin decreases the viability of the cells and with high concentrations disrupts their capability to form tube-like structures. This has also been shown earlier [15]. Defective angiogenesis can lead to and maintain a circulatory failure, *e.g.* in lower extremities predisposing to amputations [24]. Thus, our results strongly support the statement that the increased risk for minor amputations associated with current SGLT2 inhibitor therapies is most likely not a class effect. The large and long-term RCTs with different SGLT2 inhibitors also strongly support this conclusion [25]. In the CANVAS trial, canagliflozin had about a two-fold increased risk for amputations, primarily at the level of the toe or metatarsal [8], while in the large RCTs with empagliflozin and dapagliflozin this association was not detected

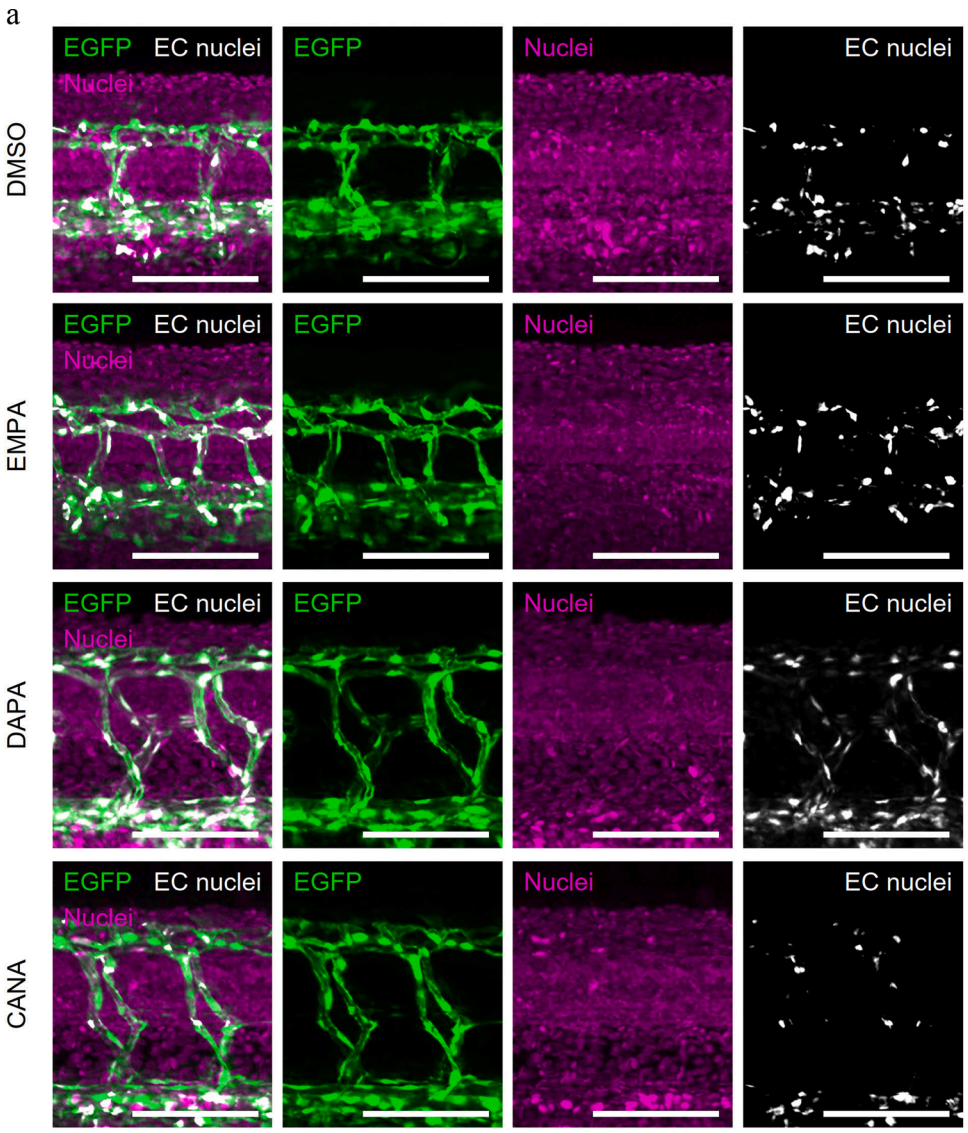

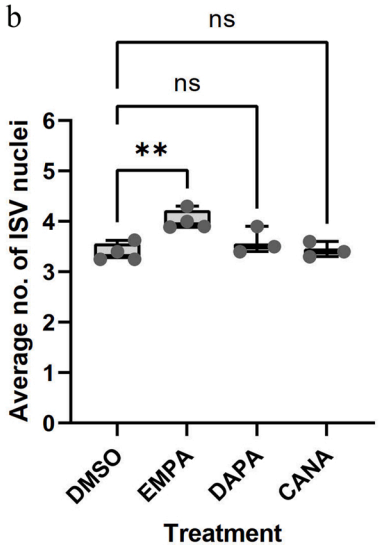

Fig. 4. 585858a Transgenic *kdrl:EGFP* zebrafish embryos were treated with SGLT2 inhibitors from 23 hpf to 54 hpf and fixed. Fixed embryos were stained for nuclei with methyl green. The samples were imaged with light-sheet fluorescence microscope. The endothelial nuclei were computationally identified through colocalization between general nuclear signal and vascular EGFP signal. Representative images are shown. Scale bar 100 μM.(4b) Quantification of the number of endothelial nuclei in ISVs. DMSO, n = 4 embryos (34 ISVs); EMPA (50 μM empagliflozin), n = 4 embryos (39 ISVs); DAPA (50 μM dapagliflozin), n = 3 embryos (23 ISVs); CANA (50 μM canagliflozin), n = 3 embryos (30 ISVs). Embryos from the same set as in experiments in Fig. 3 were used in the analysis. Statistical analysis was performed with one-way ANOVA and Dunnett's *post hoc* test. **P < 0.01, ns=non-significant.

Table 1
Number of differentially expressed genes (FC > 2 and FDR < 0.05) of zebrafish embryos after treatment with different SGLT2 inhibitors. The number of samples in each treatment group (Empagliflozin, Canagliflozin and Control) was 4.

Comparisons	Total	Upregulated	Downregulated
Empagliflozin *vs.* Control	8	4	4
Canagliflozin *vs.* Control	0	0	0
Empagliflozin *vs.* Canagliflozin	45	33	12

[11–13, 17].

It can be argued that the concentrations of the SGLT2 inhibitors used in this study were too high, because it has been shown that the maximal concentration for empagliflozin and dapagliflozin is around 0.5 μM and for canagliflozin about 3 μM [26–28]. However, in zebrafish embryo experiments of the present study, the SGLT2 inhibitors were administered into the culture medium and not directly into the embryos. The drug concentrations in the medium outside the zebrafish embryo typically exceed the within embryo concentrations as the embryo surface forms a barrier for drug uptake and bioavailability for intracellular drug targets. Often the lack of appropriate analytical methods prevents the measurement of drug concentration inside embryos, but some successfully measured examples include 5 % uptake of morphine [29] and 0.1–2 % uptake of estradiol [30]. Here, we did not have access to appropriate and validated analytical (e.g., HPLC-MS) assay to measure the actual intra-embryo concentrations of the SGLT2 inhibitors. Thus, we had to rely on the estimates mentioned above. Based on this and using estimated 0.1–5 % uptake, the effective concentration of 10 μM of empagliflozin would translate into 0.01–0.5 μM intra-embryo concentrations, and on the other hand, the 50 μM canagliflozin concentration would translate into 0.05–2.5 μM. These estimations imply that the effective concentrations of empagliflozin, dapagliflozin and canagliflozin within the embryos were at the clinically relevant range in this study.

Zebrafish is a widely recognized model for studying angiogenesis, and functional studies have shown that the molecular agents regulating vascular development are markedly conserved between fish and mammals [31–33]. The ISVs are formed through angiogenic endothelial

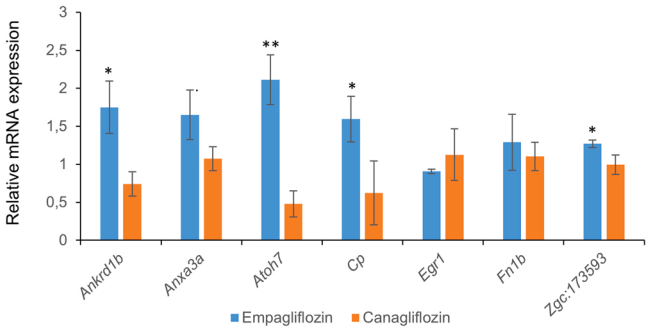

Fig. 5. Upregulated gene expression in response to SGLT2 inhibitor treatments. For each gene n = 3. The results shown are representatives of three separate experiments. Data were analyzed with Student's t-test (false discovery rate Q adjusted to 5%) and shown as mean + SD. **P < 0.01, *P < 0.05.

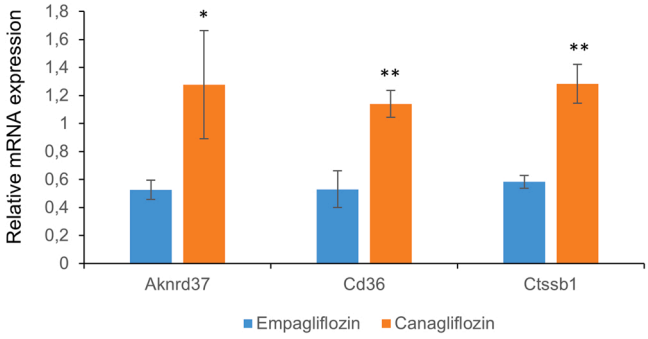

Fig. 6. Downregulated gene expression in response to SGLT2 inhibitor treatments. For each gene n = 3. The results shown are representatives of three separate experiments. Data were analyzed with Student's t-test (false discovery rate Q adjusted to 5 and shown as mean + SD. **P < 0.01, *P < 0.05.

Table 2
(A.) Angiogenesis-associated genes upregulated in zebrafish embryos in response to empagliflozin compared to canagliflozin.

Symbol	Gene zebrafish	Orthologous to human gene	Entrez ID	log2fc	Function of the gene product in angiogenesis
ankrd1b	*ankyrin repeat domain 1b*	*ANKRD1*	564159	**1.052**	Induces angiogenesis during wound healing
anxa3	*annexin A3a*	*ANXA3*	447893	**1.095**	Required during early vascular development
atoh7	*atonal bHLH transcription factor 7*	*ATOH7*	58216	**1.387**	Involved in retinal angiogenesis and vessel pattering
cp	*ceruloplasmin*	*CP*	84702	**1.256**	Induces corneal angio-genesis when bound to copper
egr1	*early growth response 1*	*EGR1*	30498	**1.096**	Induces vascular inflammation in gestational diabetes mellitus; Inhibits angiogenesis in normoxia, and induces angiogenesis in hypoxia
fn1b	*fibronectin 1b*	*FN1*	334613	**1.040**	Required for proper capillary morphogenesis and maintenance of vascular homeostasis
zgc:173593	*ferritin, heavy polypeptide-like 30*	None identified. Predicted to have ferric iron binding activity	NA	**1.162**	Proangiogenic molecule by antagonizing two-chain high mol. weight kininogen

Table 2
(B). Angiogenesis-associated genes downregulated in zebrafish embryos in response to empagliflozin compared to canagliflozin.

Symbol	**Gene zebrafish**	**Orthologous to human gene**	**Entrez ID**	**log2fc**	**Function of the gene product in angiogenesis**
ankrd37	*ankyrin repeat domain 37*	*ANKRD37*	793783	**-1.414**	Angiogenesis-related gene
cd36	*cd36 molecule*	*CD36*	436636	**-1.108**	Promotion of tumor angiogenesis
ctssb1	*cathepsin S*	*CTSS* (Cathepsin S)	554157	**-1.258**	Promotes angiogenesis; Mediator of endothelial dysfunction-related microvascular diabetes complications
mmp13a	*matrix metallopeptidase 13a*	*MMP13*	387293	**-1.060**	Induces angiogenesis related to wound healing; Involved in vascular remodeling

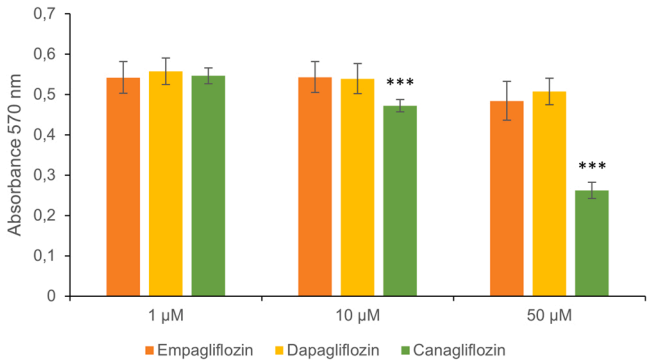

Fig. 7. Cell viability in response to SGLT2 inhibitor treatments using the MTT assay. The effect of canagliflozin and empagliflozin were compared with treatments with respective concentrations of empagliflozin (n = 3 for each treatment). The results shown are representatives of three separate experiments. Data were presented as mean + SD. *** $P < 0.001$.

sprouting, approximately starting at 22 hpf [34]. In our study, we initiated drug treatments at 23 hpf, right after the onset of ISV growth. By using this model not mimicking diabetic conditions, our results indicate remarkable regulation of angiogenic processes in non-diabetic conditions *in vivo*.

We found no clear indication of genes regulating angiogenesis using Panther analysis (Figure S1 A). Similarly, String analysis did not reveal significant molecular interactions regarding angiogenesis and vascular formation (Figure S1 B). However, we revealed several potential angiogenesis regulating candidate genes. Of the upregulated and validated genes, *ankrd1b*, *atoh7*, *cp* and *zgc:173593* have earlier been linked to various angiogenic processes. First, the expression of *ankrd1b* (alias *carp*), is associated with the regulation and initiation of arterial development in mice and rabbits [35]. It is also involved in therapeutic wound healing in ischemic wounds in rats and excisional wounds in rabbits [36]. Regarding Atoh7, its expression together with the astrocytic network is required for proper retinal vascularization and vessel patterning [37]. This is in concordance with our Panther results indicating several sequential processes in the development of the eye. Interestingly, SGLT2 inhibitors have already shown potential beneficial effects in the treatment of diabetic retinopathy and retinal microcirculation [38].

The third angiogenic candidate, Cp, has also been indicated to be an inducer of angiogenesis in the eye, namely in the capillary formation in the cornea [39]. According to our knowledge, no studies have explored the association between SGLT2 inhibitors and corneal angiogenesis. The fourth gene, zebrafish *zgc:173593*, has no orthologous human gene but is predicted to have both ferric acid iron and ferrous iron binding activities similar to ferritin. Ferritin binds to the cleaved high molecular weight kininogen, a protein with antiangiogenic properties on ECs *in vitro* and *in vivo*, and blocks its function [40].

Of the significantly downregulated and validated genes, *ankrd37* is recognized as a hypoxia-inducible factor-1 (HIF-1) target gene [41]. Like for Cd36, Ankrd37 is present in microvascular ECs and mediates the antiangiogenic effects of thrombospondin-1 [42]. Finally, *ctssb1*, orthologous to *the human cathepsin S (CTSS)*, is involved in the development and progression of *e.g.*, abdominal aortic aneurysm (AAA) [43]. Interestingly, cathepsin S also identifies as an activator of the protease-activated receptor-2 (PAR2), a receptor inducing EC injury and microvascular permeability [44].

It is well known that Vegfaa/Vegfr2 pathway plays an important role for ISV formation in zebrafish [45]. However, in the present study transcriptome analysis did not reveal any difference between SGLT2 inhibitors empagliflozin, dapagliflozin and canagliflozin in their effects on the *vegfaa/vegfr2* expression.

In addition to the *in vivo* zebrafish model, we examined the effects of SGLT2 inhibitors on the viability and sprouting of HUVECs. Consequently, we detected significant effects after treatment with canagliflozin; especially higher concentrations of canagliflozin decreased the viability of the HUVECs and disrupted their capability to form tube-like structures *in vitro*. These results confirm our *in vivo* observations on the distinctive effects of SGLT2 inhibitors on the process of angiogenesis.

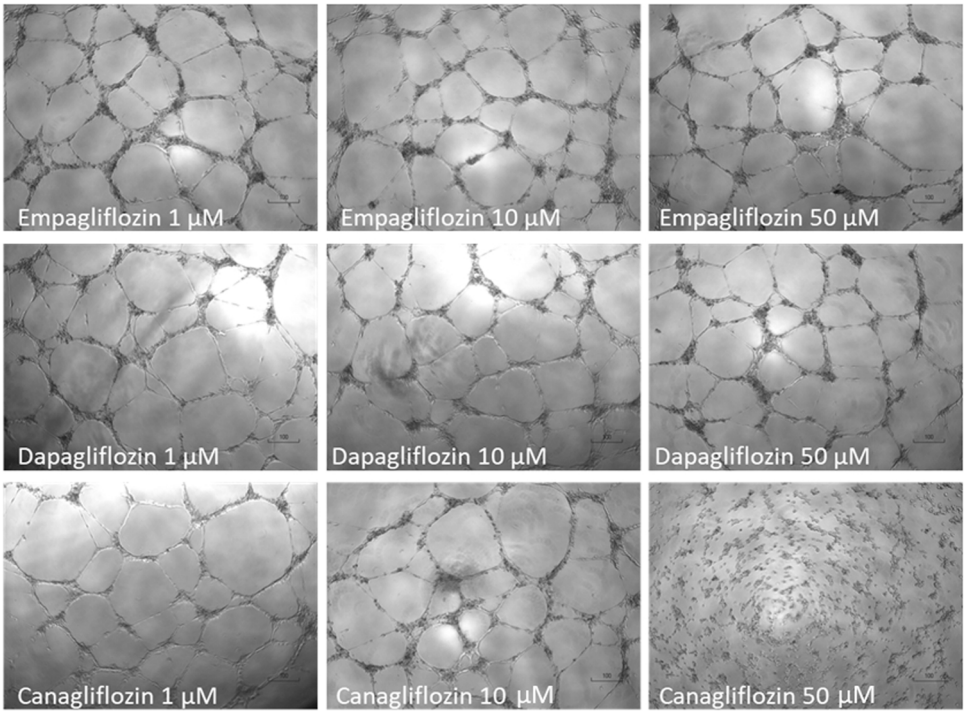

Fig. 8. Representative images of tube-formation of cultured HUVECs in response to SGLT2 inhibitor treatments. Note, that canagliflozin at the concentration of 50 µM disrupted the tube-forming capability of the cells.

5. Conclusion

In conclusion, since decreased perfusion is linked to lower-limb amputation, the differential angiogenic properties may explain variation in lower-limb amputation rates in SGLT2 inhibitor-treated patients observed in the large RCTs [7, 8, 11–13]. Although more studies are still required, clinicians should pay attention to the selection of the SGLT2 inhibitor, particularly in patients at high risk for amputation [46]. Alternatively, a more intensive follow-up of these patients would be recommendable. Based on the results of our present study and the large RCTs, namely CANVAS [47], EMPA-REG-OUTCOME [48] and DECLARE-TIMI 58 [49] the above recommendations have to be taken into consideration particularly when initiating canagliflozin therapy. Finally, the results of our present study open potential avenues for discovering new putative factors responsible for the pleiotrophic effects of SGLT2 inhibitors.

Funding

Kyllikki and Uolevi Lehikoinen Foundation, K. Albin Johanssońs foundation, Finnish Cultural Foundation, and Maud Kuistila Memorial Foundation (AS). Finnish Diabetes Research Foundation and the Research Fund of Satakunta Hospital District (HJ).

CRediT authorship contribution statement

AS co-designed the study, collected, analyzed and interpreted the data, and drafted the initial manuscript. RH analyzed and interpreted the data, and reviewed and edited to finalize the present manuscript. AH collected and analyzed the data. A-M H-S collected and analyzed the data during the revision process of the manuscript. PR took care of data curation. JM interpreted the data and drafted the initial manuscript. IP co-designed the study, analyzed and interpreted the data. HJ supervised and designed the study, interpreted the data, and drafted the initial and the revised manuscript.

Declaration of Competing Interest

The authors declare that they have no known competing financial interests or personal relationships that could have appeared to influence the work reported in this paper.

Data availability

Data will be made available on request.

Acknowledgments

This study was supported by the Finnish Functional Genomics Center, University of Turku, and Åbo Akademi and Biocenter Finland. We also thank the Medical Bioinformatics Center of Turku Bioscience Center for the analysis of the sequencing data. This Center is supported by the University of Turku, Åbo Akademi University, Biocenter Finland, and Elixir-Finland. We also thank Zebrafish Core (Turku Bioscience Center) supported by Biocenter Finland.

Appendix A. Supporting information

Supplementary data associated with this article can be found in the online version at doi:10.1016/j.biopha.2022.113882.

References

[1] D.K. McGuire, W.J. Shih, F. Cosentino, B. Charbonnel, D.Z.I. Cherney, S. Dagogo-Jack, R. Pratley, M. Greenberg, S. Wang, S. Huyck, I. Gantz, S.G. Terra, U. Masiukiewicz, C.P. Cannon, Association of SGLT2 inhibitors with cardiovascular and kidney outcomes in patients with type 2 diabetes: a meta-analysis, JAMA Cardiol. 6 (2) (2021) 148–158.

[2] B.L. Neuen, T. Young, H.J.L. Heerspink, B. Neal, V. Perkovic, L. Billot, K. W. Mahaffey, D.M. Charytan, D.C. Wheeler, C. Arnott, S. Bompoint, A. Levin, M. J. Jardine, SGLT2 inhibitors for the prevention of kidney failure in patients with type 2 diabetes: a systematic review and meta-analysis, Lancet Diabetes Endocrinol. 7 (11) (2019) 845–854.

[3] T.A. Zelniker, S.D. Wiviott, I. Raz, K. Im, E.L. Goodrich, M.P. Bonaca, O. Mosenzon, E.T. Kato, A. Cahn, R.H.M. Furtado, D.L. Bhatt, L.A. Leiter, D.K. McGuire, J.P. H. Wilding, M.S. Sabatine, SGLT2 inhibitors for primary and secondary prevention of cardiovascular and renal outcomes in type 2 diabetes: a systematic review and meta-analysis of cardiovascular outcome trials, Lancet 393 (10166) (2019) 31–39.

[4] D.C. Wheeler, B.V. Stefánsson, N. Jongs, G.M. Chertow, T. Greene, F.F. Hou, J.J. V. McMurray, R. Correa-Rotter, P. Rossing, R.D. Toto, C.D. Sjöström, A. M. Langkilde, H.J.L. Heerspink, D.-C.T.C.a. Investigators, Effects of dapagliflozin on major adverse kidney and cardiovascular events in patients with diabetic and non-diabetic chronic kidney disease: a prespecified analysis from the DAPA-CKD trial, Lancet Diabetes Endocrinol. 9 (1) (2021) 22–31.

[5] M. Packer, S.D. Anker, J. Butler, G. Filippatos, S.J. Pocock, P. Carson, J. Januzzi, S. Verma, H. Tsutsui, M. Brueckmann, W. Jamal, K. Kimura, J. Schnee, C. Zeller, D. Cotton, E. Bocchi, M. Böhm, D.J. Choi, V. Chopra, E. Chuquiure, N. Giannetti, S. Janssens, J. Zhang, J.R. Gonzalez Juanatey, S. Kaul, H.P. Brunner-La Rocca, B. Merkely, S.J. Nicholls, S. Perrone, I. Pina, P. Ponikowski, N. Sattar, M. Senni, M. F. Seronde, J. Spinar, I. Squire, S. Taddei, C. Wanner, F. Zannad, Cardiovascular and renal outcomes with empagliflozin in heart failure, N. Engl. J. Med. 383 (15) (2020) 1413–1424 (E.-R.T. Investigators).

[6] C.P. Cannon, R. Pratley, S. Dagogo-Jack, J. Mancuso, S. Huyck, U. Masiukiewicz, B. Charbonnel, R. Frederich, S. Gallo, F. Cosentino, W.J. Shih, I. Gantz, S.G. Terra, D.Z.I. Cherney, D.K. McGuire, V.C. Investigators, Cardiovascular outcomes with ertugliflozin in type 2 diabetes, N. Engl. J. Med. 383 (15) (2020) 1425–1435.

[7] B. Zinman, C. Wanner, J.M. Lachin, D. Fitchett, E. Bluhmki, S. Hantel, M. Mattheus, T. Devins, O.E. Johansen, H.J. Woerle, U.C. Broedl, S.E. Inzucchi, Empagliflozin, cardiovascular outcomes, and mortality in type 2 diabetes, N. Engl. J. Med. 373 (22) (2015) 2117–2128 (E.-R.O. Investigators).

[8] B. Neal, V. Perkovic, D.R. Matthews, Canagliflozin and cardiovascular and renal events in type 2 diabetes, N. Engl. J. Med. 377 (21) (2017) 2099.

[9] S.D. Wiviott, I. Raz, M.P. Bonaca, O. Mosenzon, E.T. Kato, A. Cahn, M. G. Silverman, T.A. Zelniker, J.F. Kuder, S.A. Murphy, D.L. Bhatt, L.A. Leiter, D. K. McGuire, J.P.H. Wilding, C.T. Ruff, I.A.M. Gause-Nilsson, M. Fredriksson, P. A. Johansson, A.M. Langkilde, M.S. Sabatine, Dapagliflozin and cardiovascular outcomes in type 2 diabetes, N. Engl. J. Med. 380 (4) (2019) 347–357 (D.T. Investigators).

[10] G.D. Lopaschuk, S. Verma, Mechanisms of cardiovascular benefits of sodium glucose co-transporter 2 (SGLT2) inhibitors: a state-of-the-art review, JACC Basic Transl. Sci. 5 (6) (2020) 632–644.

[11] S.E. Inzucchi, H. Iliev, E. Pfarr, B. Zinman, Empagliflozin and assessment of lower-limb amputations in the EMPA-REG OUTCOME Trial, Diabetes Care 41 (1) (2018) e4–e5.

[12] C. Pollock, B. Stefánsson, D. Reyner, P. Rossing, C.D. Sjöström, D.C. Wheeler, A. M. Langkilde, H.J.L. Heerspink, Albuminuria-lowering effect of dapagliflozin alone and in combination with saxagliptin and effect of dapagliflozin and saxagliptin on glycaemic control in patients with type 2 diabetes and chronic kidney disease (DELIGHT): a randomised, double-blind, placebo-controlled trial, Lancet Diabetes Endocrinol. 7 (6) (2019) 429–441.

[13] M.P. Bonaca, S.D. Wiviott, T.A. Zelniker, O. Mosenzon, D.L. Bhatt, L.A. Leiter, D. K. McGuire, E.L. Goodrich, R.H. De Mendonca Furtado, J.P.H. Wilding, A. Cahn, I. A.M. Gause-Nilsson, P. Johanson, M. Fredriksson, P.A. Johansson, A.M. Langkilde, I. Raz, M.S. Sabatine, Dapagliflozin and cardiac, kidney, and limb outcomes in patients with and without peripheral artery disease in DECLARE-TIMI 58, Circulation 142 (8) (2020) 734–747.

[14] O.H.Y. Yu, S. Dell'Aniello, B.R. Shah, V.C. Brunetti, J.M. Daigle, M. Fralick, A. Douros, N. Hu, S. Alessi-Severini, A. Fisher, S.C. Bugden, P.E. Ronksley, K. B. Filion, P. Ernst, L.M. Lix, Sodium-glucose cotransporter 2 inhibitors and the risk of below-knee amputation: a multicenter observational study, Diabetes Care 43 (10) (2020) 2444–2452 (C.N.f.O.D.E.S.C. Investigators).

[15] G. Behnammanesh, Z.E. Durante, K.J. Peyton, L.A. Martinez-Lemus, S.M. Brown, S. B. Bender, W. Durante, Canagliflozin inhibits human endothelial cell proliferation and tube formation, Front. Pharmacol. 10 (2019) 362.

[16] M. Nalugo, N. Harroun, C. Li, L. Belaygorod, C.F. Semenkovich, M.A. Zayed, Canagliflozin impedes ischemic hind-limb recovery in the setting of diabetes, Vasc. Med. 26 (2) (2021) 131–138.

[17] H. Zhou, S. Wang, P. Zhu, S. Hu, Y. Chen, J. Ren, Empagliflozin rescues diabetic myocardial microvascular injury via AMPK-mediated inhibition of mitochondrial fission, Redox Biol. 15 (2018) 335–346.

[18] S.-W. Jin, D. Beis, T. Mitchell, J.-N. Chen, D.Y.R. Stainier, Cellular and molecular analyses of vascular tube and lumen formation in zebrafish, Development 132 (23) (2005) 5199–5209.

[19] J. Schindelin, I. Arganda-Carreras, E. Frise, V. Kaynig, M. Longair, T. Pietzsch, S. Preibisch, C. Rueden, S. Saalfeld, B. Schmid, J.Y. Tinevez, D.J. White, V. Hartenstein, K. Eliceiri, P. Tomancak, A. Cardona, Fiji: an open-source platform for biological-image analysis, Nat. Methods 9 (7) (2012) 676–682.

[20] S.A. Bustin, V. Benes, J.A. Garson, J. Hellemans, J. Huggett, M. Kubista, R. Mueller, T. Nolan, M.W. Pfaffl, G.L. Shipley, J. Vandesompele, C.T. Wittwer, The MIQE guidelines: minimum information for publication of quantitative real-time PCR experiments, Clin. Chem. 55 (4) (2009) 611–622.

[21] H. Mi, A. Muruganujan, J.T. Casagrande, P.D. Thomas, Large-scale gene function analysis with the PANTHER classification system, Nat. Protoc. 8 (8) (2013) 1551–1566.
[22] D. Szklarczyk, A.L. Gable, D. Lyon, A. Junge, S. Wyder, J. Huerta-Cepas, M. Simonovic, N.T. Doncheva, J.H. Morris, P. Bork, L.J. Jensen, C.V. Mering, STRING v11: protein-protein association networks with increased coverage, supporting functional discovery in genome-wide experimental datasets, Nucleic Acids Res. 47 (D1) (2019) D607–D613.
[23] W. Durante, G. Behnammanesh, K.J. Peyton, Effects of sodium-glucose Co-transporter 2 inhibitors on vascular cell function and arterial remodeling, Int. J. Mol. Sci. 22 (16) (2021).
[24] J.A. Beckman, M.S. Duncan, S.M. Damrauer, Q.S. Wells, J.V. Barnett, D. H. Wasserman, R.J. Bedimo, A.A. Butt, V.C. Marconi, J.J. Sico, H.A. Tindle, M. P. Bonaca, A.W. Aday, M.S. Freiberg, Microvascular disease, peripheral artery disease, and amputation, Circulation 140 (6) (2019) 449–458.
[25] J. Heyward, O. Mansour, L. Olson, S. Singh, G.C. Alexander, Association between sodium-glucose cotransporter 2 (SGLT2) inhibitors and lower extremity amputation: a systematic review and meta-analysis, PLOS One 15 (6) (2020), e0234065.
[26] R. Grempler, L. Thomas, M. Eckhardt, F. Himmelsbach, A. Sauer, D.E. Sharp, R. A. Bakker, M. Mark, T. Klein, P. Eickelmann, Empagliflozin, a novel selective sodium glucose cotransporter-2 (SGLT-2) inhibitor: characterisation and comparison with other SGLT-2 inhibitors, Diabetes Obes. Metab. 14 (1) (2012) 83–90.
[27] B. Komoroski, N. Vachharajani, D. Boulton, D. Kornhauser, M. Geraldes, L. Li, M. Pfister, Dapagliflozin, a novel SGLT2 inhibitor, induces dose-dependent glucosuria in healthy subjects, Clin. Pharmacol. Ther. 85 (5) (2009) 520–526.
[28] D. Devineni, D. Polidori, Clinical pharmacokinetic, pharmacodynamic, and drug-drug interaction profile of canagliflozin, a sodium-glucose co-transporter 2 inhibitor, Clin. Pharmacokinet. 54 (10) (2015) 1027–1041.
[29] F.M. Sanchez-Simon, F.J. Arenzana, R.E. Rodriguez, In vivo effects of morphine on neuronal fate and opioid receptor expression in zebrafish embryos, Eur. J. Neurosci. 32 (4) (2010) 550–559.
[30] J.P. Souder, D.A. Gorelick, Quantification of estradiol uptake in zebrafish embryos and larvae, Toxicol. Sci. 158 (2) (2017) 465–474.
[31] E. Ellertsdóttir, A. Lenard, Y. Blum, A. Krudewig, L. Herwig, M. Affolter, H. G. Belting, Vascular morphogenesis in the zebrafish embryo, Dev. Biol. 341 (1) (2010) 56–65.
[32] N.D. Lawson, B.M. Weinstein, In vivo imaging of embryonic vascular development using transgenic zebrafish, Dev. Biol. 248 (2) (2002) 307–318.
[33] K.S. Okuda, B.M. Hogan, Endothelial cell dynamics in vascular development: insights from live-imaging in zebrafish, Front. Physiol. 11 (2020) 842.
[34] S. Isogai, N.D. Lawson, S. Torrealday, M. Horiguchi, B.M. Weinstein, Angiogenic network formation in the developing vertebrate trunk, Development 130 (21) (2003) 5281–5290.
[35] K. Boengler, F. Pipp, B. Fernandez, T. Ziegelhoeffer, W. Schaper, E. Deindl, Arteriogenesis is associated with an induction of the cardiac ankyrin repeat protein (carp), Cardiovasc Res. 59 (3) (2003) 573–581.
[36] Y. Shi, B. Reitmaier, J. Regenbogen, R.M. Slowey, S.R. Opalenik, E. Wolf, A. Goppelt, J.M. Davidson, CARP, a cardiac ankyrin repeat protein, is up-regulated during wound healing and induces angiogenesis in experimental granulation tissue, Am. J. Pathol. 166 (1) (2005) 303–312.
[37] M.L. O'Sullivan, V.M. Puñal, P.C. Kerstein, J.A. Brzezinski, T. Glaser, K.M. Wright, J.N. Kay, Astrocytes follow ganglion cell axons to establish an angiogenic template during retinal development, Glia 65 (10) (2017) 1697–1716.
[38] M. May, T. Framke, B. Junker, C. Framme, A. Pielen, C. Schindler, How and why SGLT2 inhibitors should be explored as potential treatment option in diabetic retinopathy: clinical concept and methodology, Ther. Adv. Endocrinol. Metab. 10 (2019), 2042018819891886.
[39] K.S. Raju, G. Alessandri, M. Ziche, P.M. Gullino, Ceruloplasmin, copper ions, and angiogenesis, J. Natl. Cancer Inst. 69 (5) (1982) 1183–1188.
[40] L.G. Coffman, D. Parsonage, R. D'Agostino, F.M. Torti, S.V. Torti, Regulatory effects of ferritin on angiogenesis, Proc. Natl. Acad. Sci. USA 106 (2) (2009) 570–575.
[41] Y. Benita, H. Kikuchi, A.D. Smith, M.Q. Zhang, D.C. Chung, R.J. Xavier, An integrative genomics approach identifies Hypoxia Inducible Factor-1 (HIF-1)-target genes that form the core response to hypoxia, Nucleic Acids Res. 37 (14) (2009) 4587–4602.
[42] D.W. Dawson, S.F. Pearce, R. Zhong, R.L. Silverstein, W.A. Frazier, N.P. Bouck, CD36 mediates the In vitro inhibitory effects of thrombospondin-1 on endothelial cells, J. Cell Biol. 138 (3) (1997) 707–717.
[43] Y. Qin, X. Cao, J. Guo, Y. Zhang, L. Pan, H. Zhang, H. Li, C. Tang, J. Du, G.P. Shi, Deficiency of cathepsin S attenuates angiotensin II-induced abdominal aortic aneurysm formation in apolipoprotein E-deficient mice, Cardiovasc Res 96 (3) (2012) 401–410.
[44] S. Kumar Vr, M.N. Darisipudi, S. Steiger, S.K. Devarapu, M. Tato, O.P. Kukarni, S. R. Mulay, D. Thomasova, B. Popper, J. Demleitner, G. Zuchtriegel, C. Reichel, C. D. Cohen, M.T. Lindenmeyer, H. Liapis, S. Moll, E. Reid, A.W. Stitt, B. Schott, S. Gruner, W. Haap, M. Ebeling, G. Hartmann, H.J. Anders, Cathepsin S cleavage of protease-activated receptor-2 on endothelial cells promotes microvascular diabetes complications, J. Am. Soc. Nephrol. 27 (6) (2016) 1635–1649.
[45] C.M. Toselli, B.M. Wilkinson, J. Paterson, T.J. Kieffer, Vegfa/vegfr2 signaling is necessary for zebrafish islet vessel development, but is dispensable for beta-cell and alpha-cell formation, Sci. Rep. 9 (1) (2019) 3594.
[46] U.K. Association, UK Kidney Association clinical practice guideline: sodium-glucose co-transporter-2 (SGLT-2) inhibition in adults with kidney disease. Bristol: UKKA, 2021. Available at: ukkidney.org/sites/renal.org/files/UKKA guideline_ SGLT2i in adults with kidney disease v1 18.10.21.pdf, 2021. https://www.guidelines.co.uk/renal-conditions/ukka-sglt-2-inhibition-in-adults-with-kidney-disease-guideline/456676.article. (Accessed 19th April 2022 2022).
[47] B. Neal, V. Perkovic, K.W. Mahaffey, D. de Zeeuw, G. Fulcher, N. Erondu, W. Shaw, G. Law, M. Desai, D.R. Matthews, C.P.C. Group, Canagliflozin and cardiovascular and renal events in type 2 diabetes, N. Engl. J. Med. 377 (7) (2017) 644–657.
[48] B. Zinman, S.E. Inzucchi, J.M. Lachin, C. Wanner, R. Ferrari, D. Fitchett, E. Bluhmki, S. Hantel, J. Kempthorne-Rawson, J. Newman, O.E. Johansen, H. J. Woerle, U.C. Broedl, Rationale, design, and baseline characteristics of a randomized, placebo-controlled cardiovascular outcome trial of empagliflozin (EMPA-REG OUTCOME™), Cardiovasc. Diabetol. 13 (2014) 102.
[49] I. Raz, O. Mosenzon, M.P. Bonaca, A. Cahn, E.T. Kato, M.G. Silverman, D.L. Bhatt, L.A. Leiter, D.K. McGuire, J.P.H. Wilding, I.A.M. Gause-Nilsson, A.M. Langkilde, P. A. Johansson, M.S. Sabatine, S.D. Wiviott, DECLARE-TIMI 58: participants' baseline characteristics, Diabetes Obes. Metab. 20 (5) (2018) 1102–1110.